Validation of a non-invasive fluorescence imaging system to monitor dermatological PDT

Jessica Tyrrell, BSc[1], Sandra Campbell, MD[1] and Alison Curnow, PhD[1]*

[1]Clinical Photobiology, Peninsula Medical School, University of Exeter, Knowledge Spa, Royal Cornwall Hospital, Truro, Cornwall, TR1 3HD, UK

***Corresponding author**

Telephone: 00 44 (0)1872 256432

Fax: 00 44 (0)1872 256497

E-mail: alison.curnow@pms.ac.uk

Short title: Fluorescence monitoring of dermatological PDT

Keywords: Dermatology; Fluorescence diagnosis (FD); Non-invasive fluorescence imaging; Metvix®; Methyl-aminolevulinate (MAL); Photodynamic therapy (PDT).

Abbreviations: AK, actinic keratosis; ALA, 5-aminolaevulinic acid; BCC, basal cell carcinoma; MAL, methyl-aminolevulinate; PpIX, protoporphyrin IX

Abstract

Background

Methyl-aminolevulinate (MAL) photodynamic therapy (PDT) involves selective accumulation of a photosensitiser, protoporphyrin IX (PpIX), primarily in tumour tissue, which in combination with visible light and tissue oxygen results in reactive oxygen species (ROS) production and thus cellular destruction.

Methods

A non-invasive fluorescence imaging system (Dyaderm, Biocam, Germany) has been employed to acquire colour (morphological) and fluorescent (physiological) images simultaneously during dermatological PDT. This system had been previously utilised for fluorescence diagnosis, however here changes in PpIX concentration within the skin lesions and normal tissue were followed after MAL application. Measurements were also recorded from a synthetic PpIX standard.

Results

Results indicated that imaging distance, imaging angle, position of the region of interest and light conditions all altered the PpIX levels acquired from the synthetic PpIX standard. The imaging system was therefore adapted and a standard operating

procedure developed allowing reproducible images of dermatological lesions to be acquired. Different concentrations of synthetic PpIX were analysed with the system and a linear relationship was observed between the PpIX concentration and the mean greyscale value calculated for the images acquired up to 10 μM.

Conclusions

The Dyaderm imaging system can now be used reproducibly with confidence to semi-quantify PpIX (within the range of 0 to 10 μM) within dermatological lesions using the standard operating procedure derived from this work.

Introduction

Photodynamic therapy (PDT) selectively ablates abnormal tissue and it is now a widespread treatment modality for a variety of different cancers (1, 2). PDT involves the accumulation of a photosensitiser, which in combination with light and tissue oxygen result in the production of singlet oxygen and other reactive oxygen species (ROS) causing cellular destruction (3) via apoptotic and necrotic cell death pathways (4).

PDT has been used successfully to treat numerous dermatological lesions including actinic keratosis (AK), Bowen's disease (BD) and superficial basal cell carcinomas (sBCC) (5). These lesions often present treatment complications for standard treatment modalities due to their size, location or multiplicity. PDT often negates these issues and is also associated with excellent cosmesis (6). It is therefore an important treatment methodology for certain subsets of lesions within these conditions.

The treatment of dermatological lesions with PDT involves the topical application of prodrug, either 5-aminolaevulinic acid (ALA) (7) or its methyl ester (MAL) (8). The exogenously applied ALA or MAL is absorbed through the skin following topical application and becomes a substrate in the haem biosynthetic pathway, bypassing the normal negative feedback inhibition of this pathway and resulting in accumulation of haem and haem precursors (9). The intermediate compound preceding haem is the

endogenous photosensitiser protoporphyrin IX (PpIX) and therefore photosensitisation of the cells occurs (9). The preferential accumulation of PpIX in tumour tissue is primarily influenced by the disrupted stratum corneum and differences in porphobilinogen deaminase and ferrochelatase expression (10). The methyl ester of ALA (MAL; commercially Metvix®, Galderma, U.K.) is currently licensed in the U.K. for the treatment of sBCCs, AKs, and BDs, and the current consensus indicates considerable treatment success in these indications (5, 11).

The photosensitiser PpIX is activated by several wavelengths of light, with most intense absorbance occurring at 410 nm. However for clinical PDT a longer wavelength of light (635 nm) is utilised to activate the photosensitiser, as despite lower absorbance, the depth of light penetration in tissue increases at this longer wavelength, increasing the efficacy of the treatment (12).

PpIX exhibits characteristic fluorescent properties and therefore fluorescence can be used as a diagnostic tool. PpIX exhibits red fluorescence (peak wavelengths at 635 nm and 700 nm) when excited by blue light (wavelength 410 nm) and therefore cells accumulating PpIX can be identified (13, 14). Fluorescence diagnosis in ALA-PDT can aid the identification of pre-cancerous lesions and ensure the whole lesion is properly removed during tumour excision (15, 16). The fluorescent properties of PpIX could also be potentially exploited to follow the changes in PpIX concentration within the skin during PDT. Currently clinical changes in photosensitiser concentration during ALA or

MAL induced PDT are poorly understood. It is known that increasing photosensitiser levels in the treatment area results in better clinical outcomes when ALA is employed as the prodrug (9). Therefore semi-quantitative information about accumulation and dissipation of PpIX during ALA-PDT would provide an important insight into the treatment process. In particular this information may allow a more individual treatment regime to be developed depending on PpIX accumulation within the lesion. However, the ability to follow the level of PpIX within lesions throughout PDT has to date been limited by the poor reproducibility of results and numerous factors influencing fluorescence detection (17, 18). Many parameters including tissue autofluorescence, tissue detector geometry and the absorbing and scattering properties of tissue contribute to quantification errors (19).

Previous investigations into the accumulation of PpIX due to the exogenous application of ALA or MAL have utilised invasive techniques to determine the presence and concentration of the photosensitiser within the tissues. Chemical extraction from tissues followed by high performance liquid chromatography analysis (HPLC) indicated that PpIX was the predominant porphyrin present in tumour tissue treated with ALA (20, 21). As a result the concentration of PpIX accumulating within lesional skin could be determined by chemical extraction, however this would require invasive surgery and the fluctuations throughout clinical PDT could not be followed, this technique of PpIX quantification therefore has limited practical application in real-time monitoring in the clinical environment.

This investigation validates a commercially available non-invasive fluorescence imaging system (Dyaderm, Biocam, Germany). Whilst it is possible to conduct fluorescence imaging with a number of different setups (22) including non-commercial 'home made' systems (which are commonly used in pre-clinical and clinical PDT monitoring) (23-25, 8) a commercially available piece of equipment (Dyaderm) was selected here as it could be purchased internationally in a standardised format. This is important as the majority of dermatology clinics conducting PDT treatments do not have the facilities or expertise to develop their own fluorescence imaging equipment and may simply want to be able to buy a piece of equipment for this dual purpose of fluorescence diagnosis and fluorescence monitoring or indeed use an existing piece of fluorescence diagnosis equipment for this extended use (fluorescence monitoring). The fluorescence imaging system selected was employed to acquire colour and fluorescent images simultaneously and non-invasively to follow changes in PpIX levels in lesional and non-lesional skin during various time points of clinical PDT, following validation with an *in vitro* fluorescence standard. The system was validated and adapted to ensure that the changes witnessed in PpIX levels during PDT were accurate and not due to environmental or user induced artefacts. The PpIX concentration range for which this system was accurate was also considered.

Materials and Methods

Imaging Apparatus

PpIX fluorescence was recorded using a non-invasive imaging system (Dyaderm, Biocam, Germany). The system consists of a flash light (Xenon light source with a custom bandpass filter (370–440 nm)) and a 12-bit Sony charge coupled device (CCD) camera combined in one adjustable arm coupled to a Pentium IV computer equipped with custom-made image capturing software (Dyaderm Pro v2, Biocam, Germany). The flash light emits seven light pulses per second to the skin, and the light that returns to the skin is collected by the CCD camera (exposure time 100 µs) equipped with a special Schott GG 455 longpass filter which filters out the excitation light. The excited PpIX emits light in the form of fluorescence in the red spectrum; the red pixels of the CCD camera (spectral sensitivity of which at 630 nm is between 85% and 90%) are used to generate a fluorescence image. In this way, a normal coloured image and a fluorescence image can be simultaneously collected and processed by the system in real time.

Other fluorophores within the skin will also be activated by the blue light, including lipopigments and flavins. These other fluorophores as well as endogenous background levels of PpIX are accounted for in the autofluorescence image.

In Vitro Setup

In order to ensure an accurate assessment of PpIX concentration to enable its quantification during PDT it was essential to analyse various parameters to alleviate any environmental or user induced alterations in the PpIX level. To analyse the individual parameters (detailed below) the camera was initially clamped perpendicularly to a 630 nm fluorescent standard (Figure 1A) (Biocam, Germany). Various parameters were then altered and the mean greyscale values of a synthetic PpIX standard analysed. This PpIX standard was supplied by the manufacturer of the imaging system (Biocam, Germany) and simply comprised of presynthesised PpIX which had been hermetically sealed to render it inert.

Analysis of Fluorescence Images

Images from the fluorescent standard and the patients were recorded in bitmap format, to ensure that no information was lost when condensing the data. These were then exported into NIH ImageJ software (http://rsb.info.nih.gov/ij/). This enabled the raw data to be analysed without the modifications applied by the supplied Biocam software. The mean pixel intensity of the standard was then calculated for the circular region illustrated in Figure 1.

Parameters Analysed

Warm up: The system was analysed to determine whether a warm-up phase prior to image acquisition was required. Over a two hour period the standard was imaged every five minutes. This experiment was repeated on two separate days.

Light conditions: The light conditions within the room were altered and the standard was imaged multiple times for the different light conditions. The light conditions within the room were altered by changing the overhead lights and/or opening and closing the door and/or curtains.

Placement: The position of the standard under the camera lens was altered (e.g. top of field versus the centre of field etc.). Multiple images were then acquired from each location.

Imaging Distance: The camera is supplied fitted with a spacer that is three and half centimetres long. The affect of acquiring images without the spacer was analysed in terms of fluorescence intensity and quality of the image. The camera was moved in one centimetre increments away from the standard (0 – 6 cm). For each position three images were acquired and analysed in ImageJ.

Activation Time of Camera: The camera was left active acquiring images continuously for various periods of time. Two data sets were acquired in 5 second increments from

60 seconds down to zero and a second set in reverse (in 5 seconds increments from zero up to 60 seconds).

Angle: The angle between the camera and the standard was altered up to twenty degrees either side of the normal (perpendicular) angle and multiple images of the standard were acquired at each angle.

Statistical significance was determined at the $P < 0.05$ or $P < 0.01$ employing the analysis of variance (ANOVA) for multiple groups or the Student's *t*-test where only two variables were being considered.

Reproducibility

The reproducibility of the system was analysed by acquiring multiple images of the fluorescence standard attached to white card. The standard was imaged twenty-eight times and the acquired images were subsequently analysed in ImageJ. In addition the system was adapted based on the analysis of the above parameters and the images produced by the adapted system were also analysed in a similar manner. As this system was going to be employed to image patients' dermatological lesions, the reproducibility of the standard system and the adapted system was also analysed by imaging a normal human leg. The multiple images acquired were analysed in ImageJ in two ways: i) the mean greyscale values were calculated and ii) the spread of the data was analysed. In addition images were compared to the initial image. If the system was completely reproducible then the subsequent images should have been identical to

the initial image. The subsequent images were subtracted from the initial image acquired in imageJ and the resulting image's mean greyscale value was analysed.

PpIX Concentration Range

Different concentrations of synthetic PpIX ranging from 1 nM to 10 mM were set up in 96 well plates. The fluorescence produced in each well was first studied using a previously validated Synergy HT plate reader (excitation 400/30 nm, emission 630/40 nm) in our laboratory. The solutions were then analysed using the non-invasive fluorescence imaging system. A sample (10 µl) of each well was pipetted onto parafilm and placed under the camera of the Dyaderm system (which was clamped at right angles to the surface) on top of black card. Images were acquired centrally under the camera from 3.5 cm away (i.e. the spacer distance) and the lights were on within the room. Initial studies indicated narrower concentration ranges (0 – 100 µM) should be considered which were subsequently conducted and analysed in a similar manner.

Clinical Data Capture

With research ethics committee approval patients attending the photodynamic therapy clinic in the Dermatology Department, Royal Cornwall Hospital, were consented for imaging with the Dyaderm system. Images of the lesion to be treated were acquired prior to the application of Metvix, after the three hour application period and following the light irradiation period. The images were then analysed using ImageJ software to follow the changes in PpIX fluorescence within the lesion. Images of autofluorescence

were also analysed in a similar manner to determine if significant changes in autofluorescence were observed during MAL-PDT.

Results

Warm up

The warm up profile analysed the first two hours of system activation. The mean greyscale value of the standard was analysed for every image acquired in the two hour period (Figure 2). The experiment was repeated on two separate days to also determine the variability of the system on different days. The results indicated a short initial warm up phase on each occasion. In the first half an hour a significant difference was witnessed between the ten minute time intervals ($P < 0.05$). After this initial period no significant difference was seen for the remainder of the two hours ($P < 0.86$). All subsequent experimentation was therefore conducted at least thirty minutes after turning on the machine. Comparison of the two days indicated no significant variability within the system on different days ($P < 0.16$).

Light Conditions

The mean greyscale value for the standard was determined for different light conditions within our PDT clinic room. It was observed that the mean greyscale value from the standard was dependent on the light conditions within the room (Figure 3A, $P < 0.05$). The role of light conditions were then analysed further with images acquired in subtly different light conditions (Figure 3B). The light conditions were therefore standardised for the rest of the experimentation with images being acquired with the light off, door

closed and curtains closed. Initial image acquisition with patients also used this format, however it was not trivial to align the camera to exactly the same position in the dark and therefore future clinical images were acquired with the lights on, door closed and curtains closed instead as reproducible placement was considered to be critical.

Placement

The standard was imaged at different positions under the camera lens and the mean greyscale value recorded from the standard in each position was calculated. Movement of the standard from a central location under the camera resulted in a significant decrease in the mean greyscale value in all cases (Figure 4, $P < 0.01$). Care was therefore taken in all subsequent experimentation to keep the area being investigated central to the camera's imaging field.

Imaging Distance

The standard was imaged at varying distances from the camera lens and the mean greyscale value calculated. Alterations in imaging distance from the recommended 3.5 cm resulted in unfocussed images and significant differences in the mean greyscale values (Figure 5, $P < 0.05$). These data highlight the importance of using the spacer provided with the Dyaderm equipment when taking images.

Activation Time of Camera

The fluorescence standard was imaged with altering time periods of camera activation and the mean greyscale value recorded. The results indicated that the time period of camera activation did not significantly alter the PpIX level recorded from the synthetic standard (Figure 6, $P < 0.37$). The shortest camera activation feasible was therefore employed for subsequent experimentation and care was taken not to take longer than sixty seconds, as beyond this period had not been investigated.

Imaging Angle

Alteration of the camera angle resulted in a significant difference in the mean greyscale value recorded from the standard ($P < 0.05$). However, when the angle was altered there was also a small change in the distance which was not compensated for and this could also be adversely affecting the results. The change in distance from the camera to the standard was only minimal however and therefore adjustment of the imaging angle from the normal resulted in significant differences in the mean greyscale value recorded from the standard (Figure 7). Great care is therefore required to ensure all images are taken with the camera placed perpendicular to the surface being imaged. Whilst the perpendicular angle did not provide the highest level of fluorescence intensity from the standard, subsequent experimentation was carried out at a perpendicular angle as it was easier to maintain. The fluorescence intensity measured was greatest when recorded at an angle of -20 degrees from the perpendicular. It is likely that this

occurred because at this angle significant scattering from the surface of the PpIX standard was being collected.

Reproducibility

Based on the previous experiments the system was adapted and analysed for reproducibility. Due to the system's dependency on angle and the inherent difficulties of maintaining a constant angle when imaging patients the system was adapted to alleviate these issues. The modifications involved either the attachment of an angular ruler or the attachment of a combination square. The various adapted versions and the unmodified camera were utilised to acquire multiple images of the PpIX standard (28 images acquired with each modification) and a normal human leg (50 images acquired with each modification) removing and replacing the camera each time to mimic the conditions within the clinical setting. The coefficient of variance (CV) was calculated for the data and when imaging the standard a CV of 4 % was observed for all three versions (Figure 8). However, when imaging the normal human leg the version with the combination square provided the best reproducibility with a CV of 10 % in comparison with 12 % for the other two versions (Figure 9A). Additionally the subsequent images acquired of the human leg were compared to the initial image taken with the ImageJ software, by subtracting the subsequent images from the initial image. If the images were identical the mean greyscale value of the resultant image should have been zero, the combination square had a significantly lower mean for the resultant images indicating the best reproducibility (ANOVA $P < 0.05$, Figure 9B). Therefore the

combination square was utilised for subsequent patient imaging, with the exception of only a few lesions, where the lesion localisation meant that the combination square could not be placed appropriately.

PpIX Concentration Range

The PpIX range of the non-invasive fluorescence imaging system was analysed by employing synthetic solutions of PpIX. A broad concentration range (1 nM to 10 mM) was analysed with a fluorescence plate reader as well as the fluorescence imaging system (Figure 10A & B respectively). The observed plateau was due to dimerisation of PpIX at high concentrations. This needs to be considered in the clinical setting as true changes in the photosensitiser will not be observed if PpIX accumulates to a sufficient concentration to result in dimerisation. Subsequent analysis of the 0 – 10 µM range indicated a linear relationship with the mean greyscale values quantified with both the plate reader and the Dyaderm system (Figure 10C & D respectively). Although linear regression indicated that the plate reader was more accurate (Figure 10C; $r^2 = 0.99$), the imaging system still produced an acceptable degree of accuracy (Figure 10D; $r^2 = 0.91$) considering its potential to be employed non-invasively during clinical PDT.

Clinical Data

A 75 year-old male patient with actinic keratosis on his right temple (Figure 11A) was imaged at three different time points during the treatment (Figure 11B, C & D). The

images were then analysed using ImageJ software and this indicated a statistically significant increase in PpIX fluorescence ($P < 0.01$) after three hours of Metvix application as well as a statistically significant decrease in fluorescence (with PpIX concentration returning to the initially observed level; $P < 0.01$) following the irradiation of the lesion (Figure 11E). The pre–Metvix PpIX fluorescence level was found to not be significantly different to the final post irradiation PpIX fluorescence level ($P < 0.70$). The lesion was therefore observed to undergo a statistically significant change in fluorescence during PDT. A similar response has been witnessed in other actinic keratosis lesions where a detectable fluorescence change was witnessed during PDT (Figure 12A). There was large inter-patient variation resulting in the relatively large standard deviations observed. All lesions were observed to accumulate a significant increase ($P < 0.05$) in fluorescence after the three hour application of Metvix, whereas a significant decrease ($P < 0.05$) in fluorescence was observed immediately after light irradiation had finished. Autofluorescence changes were also recorded (Figure 12B) throughout PDT and no significant change was witnessed in the patients' autofluorescence ($P > 0.75$). It should be noted that autofluorescence values were subtracted from the corresponding greyscale value of the PpIX fluorescence image throughout.

Discussion

The fluorescent properties of PpIX are commonly used in dermatological fluorescence diagnosis (26, 27, 16, 18) allowing identification and complete excision of a lesion, pre-treated with MAL or ALA. However, to further understand the role of PpIX in the efficacy of clinical MAL–PDT the concentration changes of PpIX in lesional skin during the treatment need to be followed. This will provide an insight into how different lesions accumulate the photosensitiser and subsequently respond to PDT. Previous studies have indicated that greater accumulation of PpIX and subsequent photobleaching during irradiation result in greater cell kill (28, 9). Therefore the potential ability to relate changes in PpIX concentration during light irradiation to final clinical outcome may further our understanding of PDT and thus aid clinical enhancement, by developing more individualised treatment routines.

Previously attempts to follow changes in lesional fluorescence during PDT have only looked at accumulation of PpIX and numerous concerns have been raised due to lack of reproducibility of images and the sensitivity of the system (18). The non-invasive imaging system employed in this study (Dyaderm, Biocam, Germany) has been validated here to ensure that the changes in fluorescence witnessed during PDT were due in the main to actual changes in PpIX concentration alone and not user or environmental induced artefacts.

Fluctuations were witnessed in the fluorescence level of the PpIX standard employed immediately after the system had been switched on. Images of the standard acquired within the first half an hour significantly ($P < 0.05$) differed from images acquired thereafter (Figure 2), the system therefore needs to be switched on for a period of half an hour prior to the initial image acquisition to allow a sufficient warm-up period. The system has also been shown to be consistent; the warm-up profile was followed on separate days under the same conditions and no significant fluctuations were observed.

Alteration of light conditions within the room, significantly ($P < 0.05$) altered the mean greyscale value recorded from the PpIX standard (Figure 3). In particular the switching on of the overhead lights within the room significantly altered the mean greyscale values of the images. Additionally subtle variations of the light conditions within the room (by opening or closing the door and/or the curtains) also altered the mean greyscale value recorded from the standard, although not to a significant degree. When taking images from patients during PDT the light conditions within the room therefore need to be maintained and our standard protocol is now that both the door and curtains are closed (to limit the effect of external light) and the internal lights are kept on when obtaining the fluorescence images (to enable the imaging system to be aligned in exactly the same position). In light of our initial clinical data, the changes witnessed during the treatment are usually of such a sizable nature that small alterations in the external light conditions, although significant for the standard are likely to be clinically irrelevant and thus an acceptable level of error in clinical practice. It should be noted that we also routinely image the PpIX standard before and after clinical data acquisition to check that the

measurements made by the system on each day of use are as expected and to date we have observed no evidence that the PpIX standard provided with the system bleaches over extended or repeated exposures.

Variations were also witnessed in the mean greyscale value recorded from the PpIX standard when its position relative to the camera was altered (Figure 4). Images acquired from a central location under the camera lens had significantly ($P < 0.01$) increased mean greyscale values in comparison to those imaged around the periphery of the lens. Therefore care has to be taken to ensure that when lesions are imaged they are aligned centrally under the camera to ensure fluctuations in PpIX fluorescence are due to changes in the PpIX concentration alone. This is particularly important when repositioning the camera to the same lesion at different points in the PDT process.

These validation studies verified the use of the spacer (3.5 cm) provided with the imaging system. The images of the standard acquired at alternative distances away from the camera lens resulted in significant differences ($P < 0.05$) in mean greyscale values (Figure 5) and unfocused images. The spacer therefore must be in contact with the patient's skin to ensure that images are acquired at the same distance to ensure that the images are focussed and the values obtained are reproducible. It is acknowledged that in some instances the positioning of the spacer is not trivial as some lesions are not appropriately located for its easy application.

The most intense absorbance of PpIX occurs at 410 nm (12). The imaging system employed here utilises light in this region and therefore the effects of prolonged camera activation were analysed on measurements taken from the synthetic standard (Figure 6). There was no significant alteration in the mean greyscale value of the standard during periods of sixty second activation. However, due to the propensity of PpIX to be photobleached by blue light, a maximum activation limit of sixty seconds has been imposed when imaging patients. Further investigations could be conducted to consider this factor in more detail in clinical practice.

Alterations in the angle of the camera relative to the standard indicated that angular variations significantly ($P < 0.05$) altered the images acquired (Figure 7). Angular changes of as little as 5º from the normal perpendicular position significantly altered the images. The angle of the camera relative to a lesion therefore needs to be maintained. The system in our experience required slight adaptation to ensure a constant right angle as in our previous clinical experience we have found (data not shown) that there can be a large degree of human error in the placement of the camera. The first adaptation involved the addition of a combination square, which maintained a normal angle. An alternative adaptation involved the addition of an angular ruler, where the angle of placement could be altered depending on localisation. The reproducibility of the adapted versions was compared to that of the unmodified camera in the acquisition of multiple images from the standard (Figure 8) and a normal human leg (Figure 9). The initial experiments with the standard indicated little variation in the reproducibility of the different systems (CV 4 % for all systems), however it was concluded that imaging at a

constant angle would be less trivial when it came to a patient. The findings when imaging a normal human leg indicated that a lower spread of data and lower CV was seen for the combination square and that this adaptation resulted in significantly ($P < 0.05$) lower deviations of subsequent images from the initial image acquired. Consequently the combination square adaptation has been utilised when imaging patients to enhance the reproducibility of the images. Certain lesion localisations may not lend themselves to the placement of the camera at a normal angle and therefore in our experience despite no significant improvement in reproducibility, the angular ruler may occasionally need to be used to ensure placement of the camera at the same angle relative to the lesion.

The authors acknowledge that the fluorescence standard utilised here does not provide an environment comparable to skin tissue, where the optical properties of the tissue will significantly affect the attenuation of the excitation light (17, 29). However these initial investigations have enabled adaptation and development of a standard operating procedure enabling reproducible images to subsequently be obtained from normal human skin (Figure 10).

Analysis of synthetic solutions of PpIX indicated that the non-invasive imaging system quantified PpIX in a similar manner to the Synergy HT plate reader (Figure 11) albeit not to such a high degree of accuracy. A linear relationship was witnessed between the PpIX concentration of the solution and the mean greyscale values of the images

recorded by the imaging system in the 0 – 10 μM range (Figure 11D). Further analysis of the system indicated that the relationship between PpIX concentration and the mean greyscale value was not linear beyond 10 μM. Initial clinical data recorded (Figure 12) has indicated that the majority of data we collect clinically when conducting dermatological PDT does fall primarily within mean greyscale values which are linearly related to the synthetic PpIX concentration, although some PpIX values prior to light irradiation may exceed this range slightly (mean estimates of PpIX levels from these data are ~0.80 μM pre MAL application, ~10.00 μM post MAL application and ~0.75 μM post irradiation). However, the quantification of data collected clinically into actual PpIX concentrations should only be done with careful consideration. The standard curves were produced from synthetic PpIX and this does not correspond directly to images acquired *in vivo* due to the complex nature of skin tissue and the heterogeneity of PpIX within tissue (30, 31). In addition the limited penetration of blue light into deeper skin layers may cause PpIX deep within lesions to be undetectable (32). However, 410 nm light has been shown to penetrate well with greater than 70% incident light reaching depths of 0.1 – 0.15 mm and therefore the light should penetrate the depth of the epidermis where the majority of PpIX will be localised (33). The synthetic PpIX solutions demonstrated that the non-invasive imaging system does detect PpIX fluorescence and that increasing concentrations correlate to an increase in fluorescence observed with the system.

The clinical data collected were analysed and presented in the figures semi-quantitatively utilising image analysis rather than converting the images to actual PpIX

concentrations due to the aforementioned issues. To accurately determine the PpIX concentration, chemical extraction would be necessary. This has not been undertaken here but a previous study has shown a positive correlation between the *in vivo* fluorescence witnessed with the Dyaderm to biochemical tissue PpIX content (32).

Initial clinical data (Figures 11 & 12) verify the ability of the system to detect changes in PpIX fluorescence during PDT treatment. These data indicate the large changes witnessed in these actinic keratosis lesions at the various points in the treatment considered. The significant changes in PpIX witnessed within the clinical setting are crucial as they further aid the practical application of the system. Despite the importance of alleviating variations in PpIX due to user or environmental induced artefacts, the large changes witnessed clinically ensure that subtle variations that cannot be alleviated by following the standard operating procedure derived here are not clinically relevant or detrimental in this setting. The CV of the imaging system on a large area of normal human leg was calculated to be 10 % for the imaging system modified with the combination square. When monitoring real-time dermatological PDT much greater changes were observed: large increases in fluorescence intensity occurred after MAL application (> 300 % increase in the example presented here) and a correspondingly large decrease was observed following light irradiation (75 % decrease). Due to the nature of PDT, tissue autofluorescence is expected to alter during the treatment of the lesions (29). The non-invasive imaging system records autofluorescence at 410 nm at which flavins and lipopigments will provide an autofluorescence signal (34). Image analysis indicated no significant change in

autofluorescence (Figure 12B) and therefore the changes observed in fluorescence reported herein are primarily due to the accumulation/dissipation of PpIX within the lesions.

The findings from this investigation have indicated that with subtle adaptation and consistent application the Dyaderm non-invasive fluorescence imaging system can be utilised to produce reproducible measures of PpIX levels during dermatological PDT. Therefore semi-quantitative measures of PpIX within lesional and non-lesional tissue can be reproducibly determined/followed during clinical dermatological PDT in a non-invasive manner for the first time using this commercially available equipment.

Comparison of images acquired in the future, prior to the application of ALA or MAL, immediately prior to irradiation and following irradiation of the lesion with light will provide large quantities of information for analysis and detailed study. For instance this information will provide insights into whether the lesions currently licensed for treatment with Metvix all consistently accumulate PpIX and respond in the same manner to the treatment and whether other currently non-licensed dermatological conditions may also benefit from PDT treatment. In addition with further investigation the results may help to indicate relationships between changes in PpIX concentration and the final clinical outcome, as previous investigations indicate that greater PpIX photobleaching correlates to greater cell kill (27, 35). If quasi-continuous monitoring of PpIX fluorescence were to be attempted during the light period in the future however, it would

be necessary to temporarily switch off the light source in order for fluorescence images/measurements to be taken.

The ability to utilise this non-invasive fluorescence imaging system reproducibly to follow the changes in PpIX within clinical dermatological lesions could further our understanding of clinical PDT. The majority of current knowledge relating to the accumulation of PpIX in PDT comes from *in vitro* studies (36-38) rather than actual clinical application. However, the system described here can now be utilised to determine PpIX levels/changes in a non-invasive manner whilst therapeutic clinical dermatological PDT is in progress and as such is a useful advancement to the field.

Conflict of Interest

The authors state no conflict of interest.

Acknowledgements

This work was supported by the Duchy Health Charity Limited.

References

[1] Ackroyd R, Kelty C, Brown N, Reed M. The history of photodetection and photodynamic therapy. Photochem Photobiol 2001;74:656-669.

[2] Sibata CH, Colussi VC, Oleinick NL, Kinsella TJ. Photodynamic therapy: a new concept in medical treatment. Braz J Med Biol Res 2000;33:869-880.

[3] Henderson BW, Dougherty TJ. How does photodynamic therapy work? Photochem Photobiol 1992;55:145-157.

[4] Noodt BB, Berg K, Stokke T, Peng Q, Nesland JM. Apoptosis and necrosis induced with light and 5-aminolaevulinic acid-derived protoporphyrin IX. BJC 1996;74:22-29.

[5] Calzavara-Pinton PG, Venturini M, Sala R. Photodynamic therapy: update 2006. Part 2: Clinical results. J European Acad Derm Vene 2007;21:439-451.

[6] Svanberg K, Andersson T, Killander D, Wang I, Stenram U, Andersson-Engels S*, et al.* Photodynamic therapy of non-melanoma malignant tumours of the skin using topical delta-aminolevulinic acid sensitization and laser irradiation. BJD 1994;130:743-751.

[7] Malik Z, Lugaci H. Destruction of erythroleukaemic cells by photoactivation of endogenous porphyrins. BJC 1987;56:589-595.

[8] Peng Q, Soler AM, Warloe T, Nesland JM, Giercksky KE. Selective distribution of porphyrins in skin thick basal cell carcinoma after topical application of methyl 5-aminolevulinate. JPPB 2001;62:140-145.

[9] Peng Q, Berg K, Moan J, Kongshaug M, Nesland JM. 5-Aminolevulinic acid-based photodynamic therapy: principles and experimental research. Photochem Photobiol 1997;65:235-251.

[10] Peng Q, Warloe T, Berg K, Moan J, Kongshaug M, Giercksky KE*, et al.* 5-Aminolevulinic acid-based photodynamic therapy. Clinical research and future challenges. Cancer 1997;79:2282-2308.

[11] Morton CA, Brown SB, Collins S, Ibbotson S, Jenkinson H, Kurwa H*, et al.* Guidelines for topical photodynamic therapy: report of a workshop of the British Photodermatology Group. BJD 2002;146:552-567.

[12] Moan J, Iani V, Ma LW. In: Benjamin E, Giulio J, Moan J editors. Choice of the proper wavelength for photochemotherapy. SPIE 1996;544-549.

[13] Scott MA, Hopper C, Sahota A, Springett R, McIlroy BW, Bown SG*, et al.* Fluorescence Photodiagnosis and Photobleaching Studies of Cancerous Lesions using Ratio Imaging and Spectroscopic Techniques. Lasers Med Sci 2000;15:63-72.

[14] Wennberg AM, Gudmundson F, Stenquist B, Ternesten A, Molne L, Rosen A*, et al*. In vivo detection of basal cell carcinoma using imaging spectroscopy. Acta Derm Venereol 1999;79:54-61.

[15] Ackermann G, Abels C, Karrer S, Baumler W, Landthaler M, Szeimies RM. Fluorescence-assisted biopsy of basal cell carcinomas. Hautarzt 2000;51:920-924.

[16] Siewecke C, Szeimies RM. PDT and fluorescence diagnosis in dermatology. Hospital Pharmacy Europe 2004;May/June:49-52.

[17] Bogaards A, Sterenborg HJ, Trachtenberg J, Wilson BC, Lilge L. In vivo quantification of fluorescent molecular markers in real-time by ratio imaging for diagnostic screening and image-guided surgery. Lasers Surg Med 2007;39:605-613.

[18] Smits T, Kleinpenning MM, Blokx WA, van de Kerkhof PC, van Erp PE, Gerritsen MJ. Fluorescence diagnosis in keratinocytic intraepidermal neoplasias. J Am Acad Derm 2007;57:824-831.

[19] Bogaards A, Aalders MC, Zeyl CC, de Blok S, Dannecker C, Hillemanns P*, et al*. Localization and staging of cervical intraepithelial neoplasia using double ratio fluorescence imaging. J Biomed Opt 2002;7:215-220.

[20] Hua Z, Gibson SL, Foster TH, Hilf R. Effectiveness of delta-aminolevulinic acid-induced protoporphyrin as a photosensitiser for photodynamic therapy in vivo. Cancer Res 1995;55:1723-1731.

[21] Loh CS, Vernon D, MacRobert AJ, Bedwell J, Bown SG, Brown SB. Endogenous porphyrin distribution induced by 5-aminolaevulinic acid in the tissue layers of the gastrointestinal tract. JPPB 1993;20:47-54.

[22] Andersson-Engels S, Klinteberg C, Svanberg K, Svanberg S. In vivo fluorescence imaging for tissue diagnostics. Phys Med Biol 1997;42:815-824.

[23] Boere IA, Robinson DJ, de Bruijn HS, van den Boogert J, Tilanus HW, Sterenborg HJ*, et al.* Monitoring in situ dosimetry and protoporphyrin IX fluorescence photobleaching in the normal rat esophagus during 5-aminolevulinic acid photodynamic therapy. Photochem Photobiol 2003;78:271-277.

[24] Ericson MB, Sandberg C, Stenquist B, Gudmundson F, Karlsson M, Ros AM*, et al*. Photodynamic therapy of actinic keratosis at varying fluence rates: assessment of photobleaching, pain and primary clinical outcome. BJD 2004;151:1204-1212.

[25] Loschenov VB, Konov VI, Prokhorov AM. Photodynamic therapy and Fluorescence Diagnostics. Laser Physics 2000;10:1188-1207.

[26] Berg K, Selbo PK, Weyergang A, Dietze A, Prasmickaite L, Bonsted A*, et al*. Porphyrin-related photosensitizers for cancer imaging and therapeutic applications. J Microscopy 2005;218:133-147.

[27] Smits T, Kleinpenning MM, van Erp PE, van de Kerkhof PC, Gerritsen MJ. A placebo-controlled randomized study on the clinical effectiveness, immunohistochemical changes and protoporphyrin IX accumulation in fractionated 5-aminolaevulinic acid-photodynamic therapy in patients with psoriasis. BJD 2006;155:429-436.

[28] Ascencio M, Collinet P, Farine MO, Mordon S. Protoporphyrin IX fluorescence photobleaching is a useful tool to predict the response of rat ovarian cancer following hexaminolevulinate photodynamic therapy. Lasers Surg Med 2008;40:332-341.

[29] Bogaards A, Sterenborg HJ, Wilson BC. *In vivo* quantification of fluorescent molecular markers in real-time: A review to evaluate the performance of five existing methods. Photodiagnosis Photodynamic Therapy 2007;4:170-178.

[30] Kleinpenning MM, Smits T, Ewalds E, van Erp PE, van de Kerkhof PC, Gerritsen MJ. Heterogeneity of fluorescence in psoriasis after application of 5-aminolaevulinic acid: an immunohistochemical study. BJD 2006;155:539-545.

[31] Martin A, Tope WD, Grevelink JM, Starr JC, Fewkes JL, Flotte TJ*, et al.* Lack of selectivity of protoporphyrin IX fluorescence for basal cell carcinoma after topical

application of 5-aminolevulinic acid: implications for photodynamic treatment. Archives Derm Res 1995;287:665-674.

[32] Smits T, Robles CA, van Erp PE, van de Kerkhof PC, Gerritsen MJ. Correlation between macroscopic fluorescence and protoporphyrin IX content in psoriasis and actinic keratosis following application of aminolevulinic acid. J Invest Dermatol 2005;125:833-839.

[33] Anderson RR, Parrish JA. The optics of human skin. J Invest Dermatol 1981;77:13-19.

[34] Bashkatov AN, Genina EA, Kochubey VI, Tuchin VV. Optical properties of human skin, subcutaneous and mucous tissues in the wavelength range from 400 to 2000 nm. J Phys D: Appl Phys 2005;38:2543-2555.

[35] Robinson DJ, de Bruijn HS, van der Veen N, Stringer MR, Brown SB, Star WM. Fluorescence photobleaching of ALA-induced protoporphyrin IX during photodynamic therapy of normal hairless mouse skin: the effect of light dose and irradiance and the resulting biological effect. Photochem Photobiol 1998;67:140-149.

[36] Bech O, Berg K, Moan J. The pH dependency of protoporphyrin IX formation in cells incubated with 5-aminolevulinic acid. Cancer Letters 1997;113:25-29.

[37] Bedwell J, MacRobert AJ, Phillips D, Bown SG. Fluorescence distribution and photodynamic effect of ALA-induced PP IX in the DMH rat colonic tumour model. BJC 1992;65:818-824.

[38] Berg K, Anholt H, Bech O, Moan J. The influence of iron chelators on the accumulation of protoporphyrin IX in 5-aminolaevulinic acid-treated cells. BJC 1996;74:688-697.

Figure Legends

Figure 1: A photograph of the fluorescent standard with a circle indicating the region analysed in ImageJ.

Figure 2: The warm up profile of the imaging system produced by taking images of the same fluorescence standard over a two hour period on two separate days. The solid circles represent data collected on day one (linear trend indicated by solid line) and the unfilled circles represent data collected on day two (linear trend indicated by dashed line). Error bars indicate the standard deviation between the five images acquired of the standard at each time point and have been presented unidirectionally for each data set for clarity.

Figure 3: Mean greyscale values of the standard recorded when the light level within the room was altered. The dark grey bars indicate when the light was off and the light grey bars relate to when the light was switched on. A) Indicates the significant difference in mean greyscale value observed when considering the status of the overhead lights alone ($P < 0.05$) and B) indicates the alterations observed by opening and closing the door and/or curtains within the room. + indicates parameters chosen for future experimentation and ++ indicates the parameters used in the clinical acquisition of images. Error bars indicate the standard deviations of the twenty images acquired for each different light condition.

Figure 4: Bar chart illustrating the alteration of the recorded greyscale value of the PpIX standard when placed at different positions under the Dyaderm. There was a statistically significant difference in the mean greyscale value of the standard recorded (ANOVA analysis indicated difference at $P < 0.01$) between the central position and all other regions. + indicates the parameter employed for all future experimentation. Error bars indicate the standard deviation of the multiple images acquired in each position.

Figure 5: Plot indicating the alteration in mean greyscale values of the standard as the camera lens was moved further away from the fluorescence standard. + indicates distance employed when taking subsequent PpIX measurements. Error bars indicate the standard deviation of the 20 images acquired at each distance.

Figure 6: Plot indicating the alteration in mean greyscale value for increasing and decreasing periods of camera activation. The unfilled circles indicate the values taken in order from 60 s to 0 s whereas the solid circles indicate values taken in the reverse order (i.e. from 0 s to 60 s). Statistical analysis indicated there was no significant difference between the two groups ($P > 0.05$). Error bars indicate the deviation of the mean greyscale value when the experiment was repeated three times in each direction.

Figure 7: Plot indicating that the imaging angle significantly altered the recorded greyscale value from the fluorescence standard. Alterations of the camera imaging angle by as little as 5º significantly altered the mean greyscale value of the standard (ANOVA $P < 0.05$). + indicates the angle employed when taking subsequent PpIX

measurements. Error bars indicate the standard deviation of the 20 images acquired for each angular placement.

Figure 8: A) Box and whisker plot indicating the range of PpIX values obtained using the different setups to try to ensure a perpendicular imaging angle from a standard. The central line indicates the mean, the box indicates the data within the interquartile range and the whiskers indicate the standard deviations of the data with the dots representing outliers. B) Bar chart indicating the mean difference in greyscale value of subsequent images from the initial image acquired using the three different setups. The error bars indicate the standard deviation of the mean difference observed.

Figure 9: A) Box and whisker plot indicating the range of PpIX values obtained using the different setups to try to ensure a perpendicular imaging angle from a normal human leg. The central line indicates the mean observed, the box indicates the data within the interquartile range of the data and the whiskers indicate the standard deviations of the data with the dots representing outliers. B) Bar chart indicating the mean difference in greyscale value of subsequent images from the initial image acquired using the three different setups. The error bars indicate the standard deviation of the mean difference observed. The combination square was significantly more reproducible than either of the other setups investigated ($P < 0.001$) and was therefore employed in future experimentation (+).

Figure 10: Plot of PpIX fluorescence intensity versus Log PpIX concentration recorded with A) the Synergy HT plate reader and B) the fluorescence imaging system. Additionally plot of PpIX fluorescence intensity versus PpIX concentration indicating the linear regression lines for the 0 – 10 μM concentration range recorded with C) the Synergy HT plate reader and D) the fluorescence imaging system. Error bars on all panels indicate the standard deviation of five samples at each concentration.

Figure 11: A) White light image indicating an actinic keratosis lesion on a man's right temple. Images B, C, and D indicate the change in PpIX fluorescence through the PDT treatment process, where B) is the initial image acquired prior to Metvix application, C) is the fluorescence image after Metvix had been applied for three hours and D) is the fluorescence image immediately after light irradiation had been completed. The images shown (A-D) are magnified by a factor of three. E) The bar chart highlights the changes in the mean greyscale value of the fluorescence images (error bars indicate the standard deviations in the pixel intensity in the area analysed). * indicates a statistically significant difference ($P < 0.05$) in fluorescence after the application of Metvix for three hours in comparison to the initial fluorescence image and the image post irradiation.

Figure 12: A) Bar chart indicating the mean greyscale values recorded from a series of twenty different actinic keratosis lesions at different points in the treatment. The error bars indicate the standard deviations in the pixel intensity in the area analysed. Paired t-test indicated a statistically significant difference in PpIX accumulation after MAL application ($P < 0.01$) and PpIX dissipation ($P < 0.01$) after light irradiation. The large

standard deviations reflect large inter-patient variations. B) Bar chart indicating mean greyscale values for autofluorescence recorded in the twenty patients undergoing PDT.

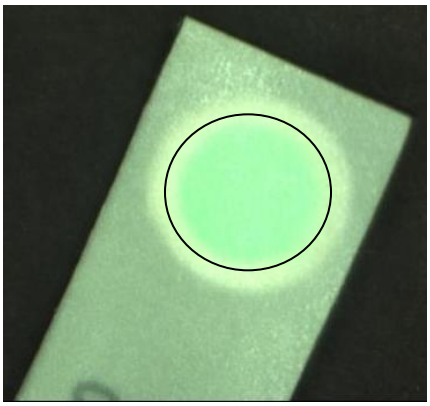

Figure 1

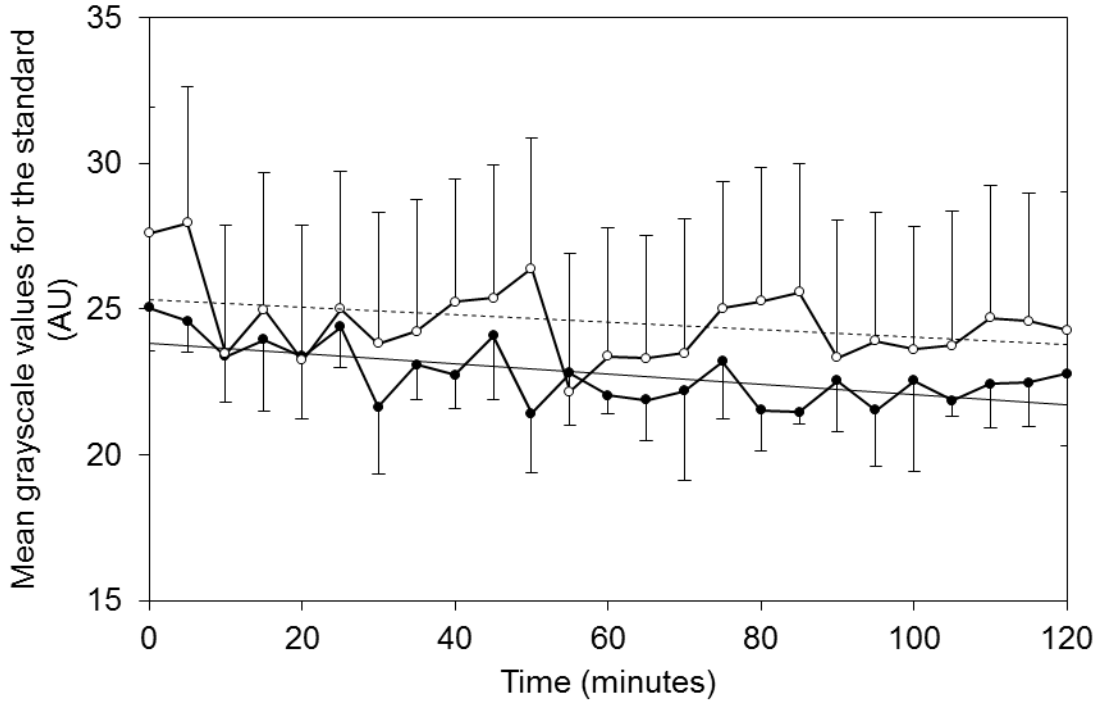
Mean grayscale values for the standard (AU)
35
30
25
20
15
0
20
40
60
80
100
120
Time (minutes)

Figure 2

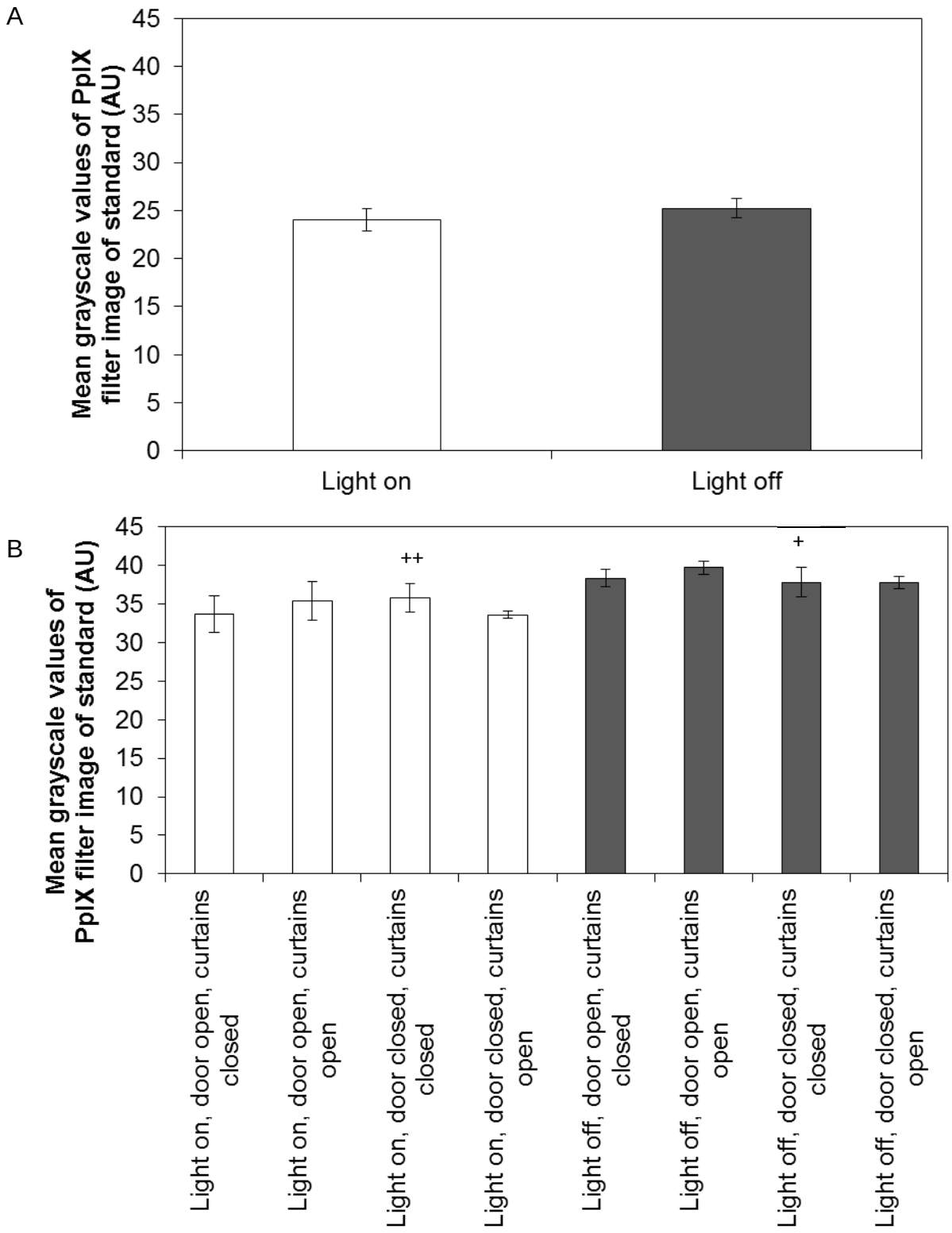
A
Mean grayscale values of PpIX filter image of standard (AU)
45
40
35
30
25
20
15
10
5
0
Light on
Light off
B
Mean grayscale values of PpIX filter image of standard (AU)
45
40
35
30
25
20
15
10
5
0
++
+
Light on, door open, curtains closed
Light on, door open, curtains open
Light on, door closed, curtains closed
Light on, door closed, curtains open
Light off, door open, curtains closed
Light off, door open, curtains open
Light off, door closed, curtains closed
Light off, door closed, curtains open

Figure 3

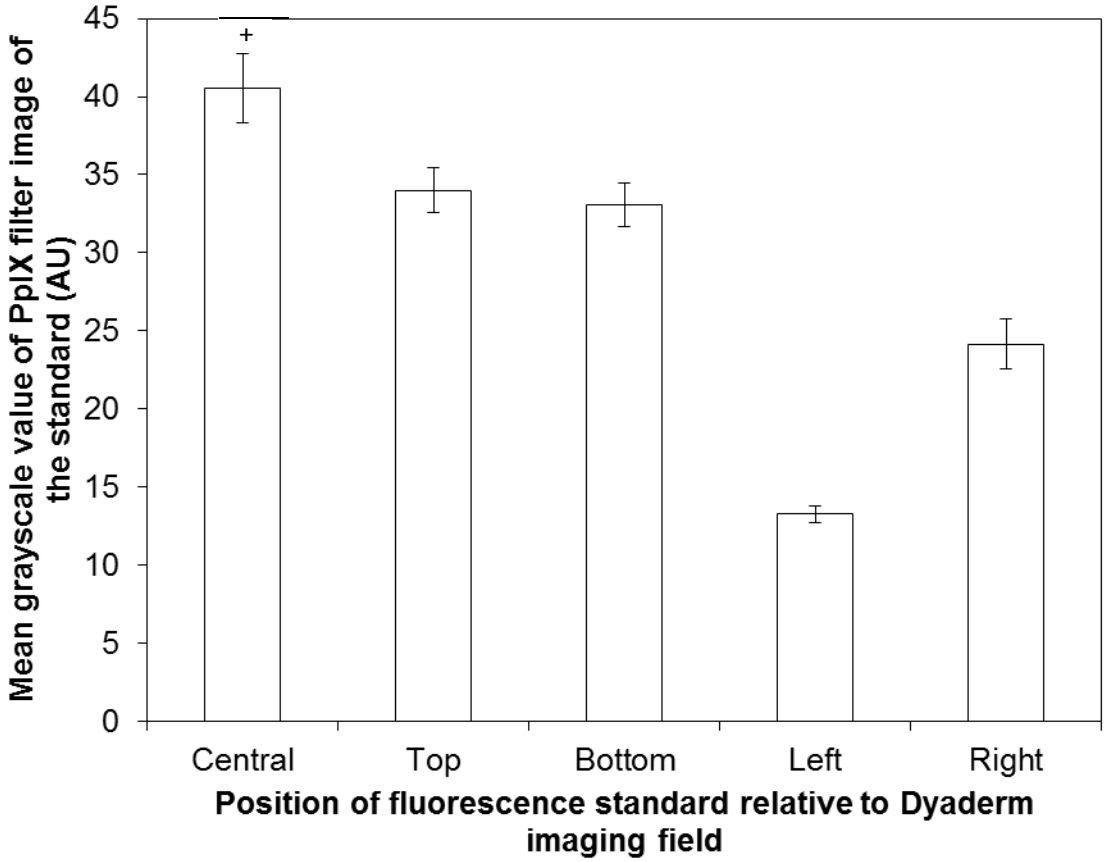
Mean grayscale value of PpIX filter image of the standard (AU)
45
40
35
30
25
20
15
10
5
0
Central
Top
Bottom
Left
Right
Position of fluorescence standard relative to Dyaderm imaging field

Figure 4

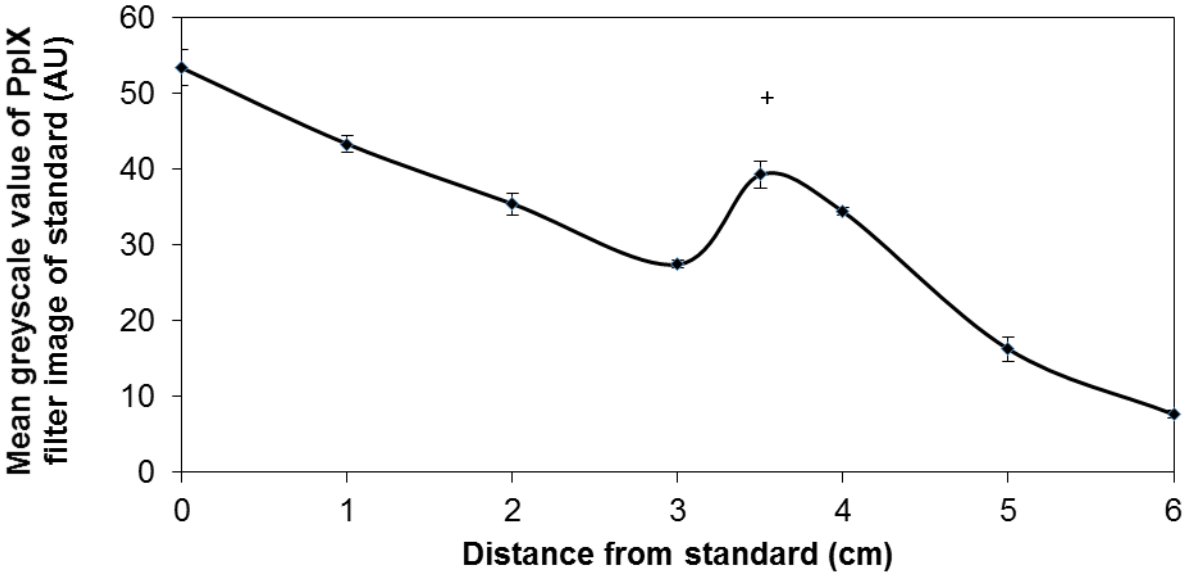
Mean greyscale value of PpIX filter image of standard (AU)
60
50
40
30
20
10
0
0
1
2
3
4
5
6
Distance from standard (cm)

Figure 5

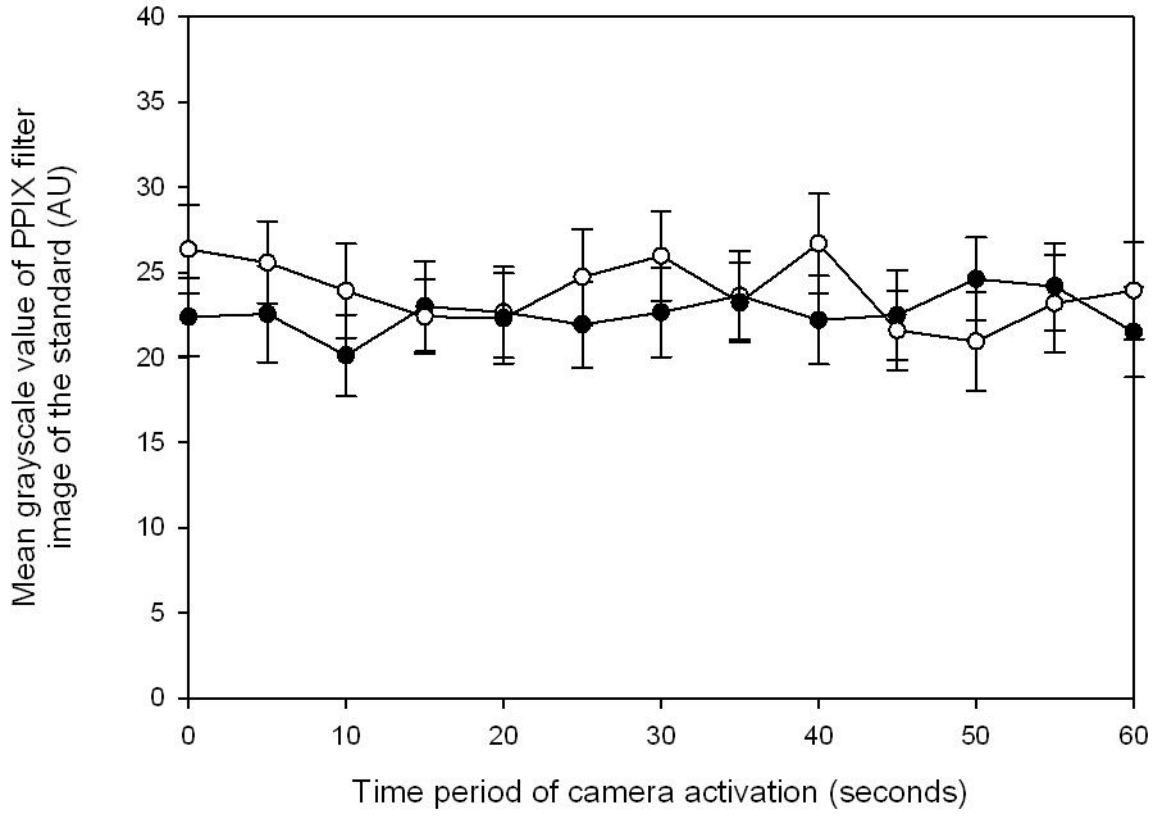
Mean grayscale value of PPIX filter image of the standard (AU)
40
35
30
25
20
15
10
5
0
0
10
20
30
40
50
60
Time period of camera activation (seconds)

Figure 6

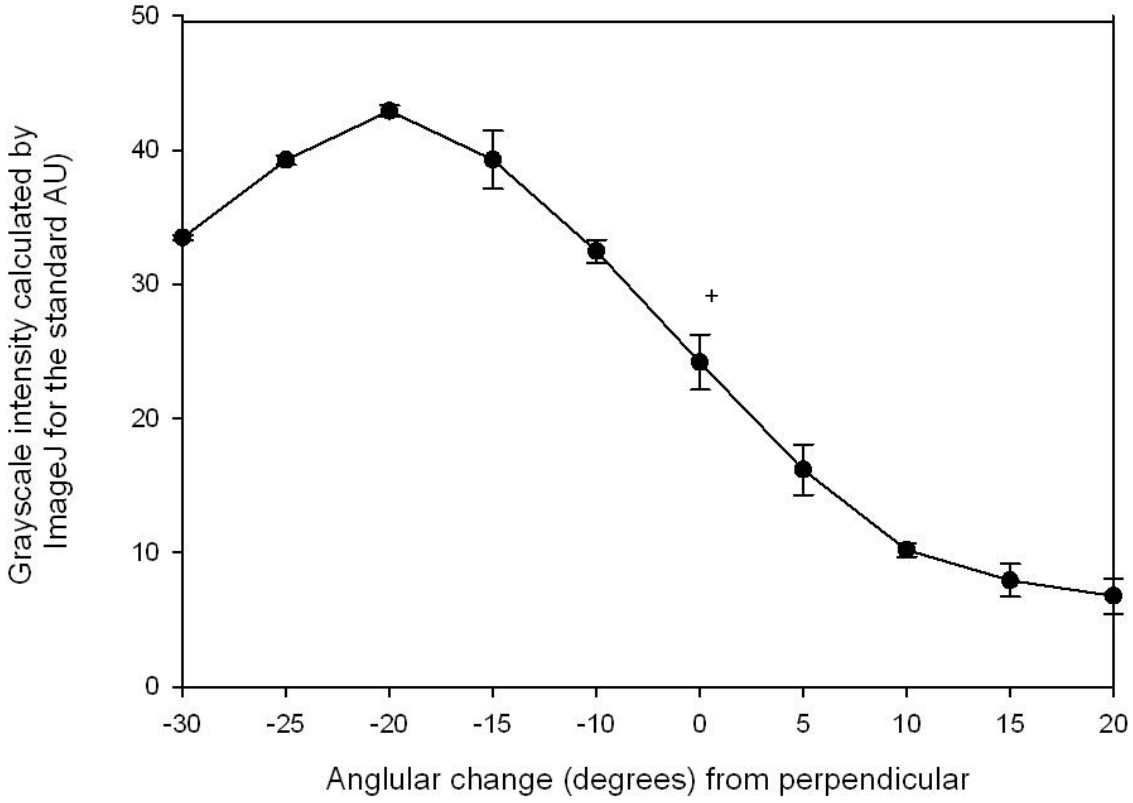
Grayscale intensity calculated by ImageJ for the standard AU)
50
40
30
20
10
0
-30
-25
-20
-15
-10
0
5
10
15
20
Anglular change (degrees) from perpendicular

Figure 7

A

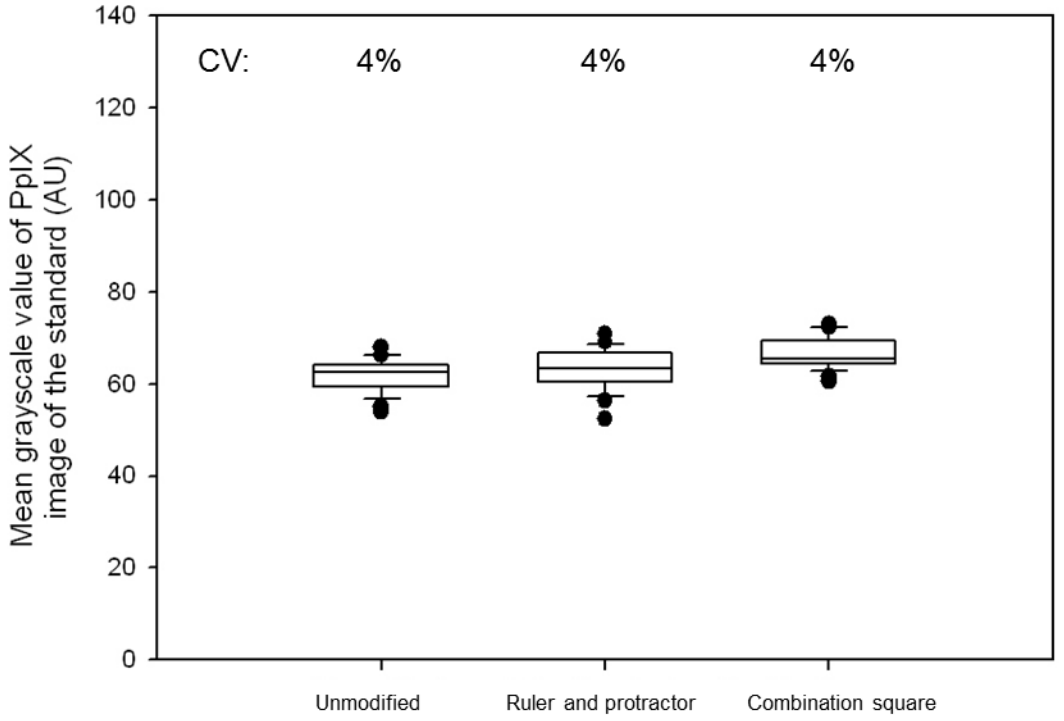
CV:
4%
4%
4%
Mean grayscale value of PpIX image of the standard (AU)
140
120
100
80
60
40
20
0
Unmodified
Ruler and protractor
Combination square

B

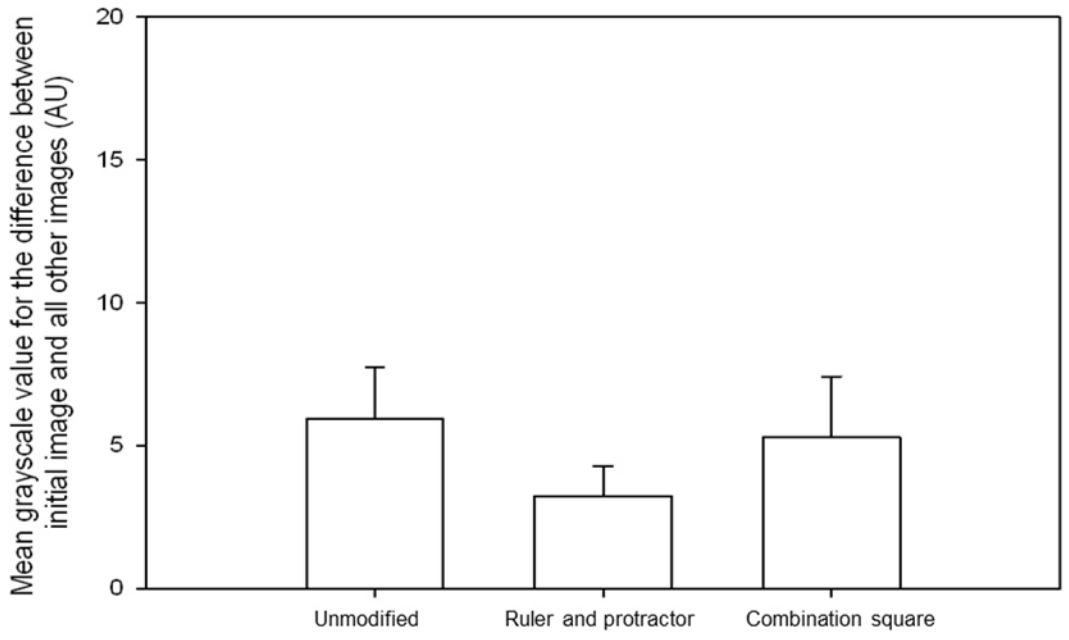
Mean grayscale value for the difference between initial image and all other images (AU)
20
15
10
5
0
Unmodified
Ruler and protractor
Combination square

Figure 8

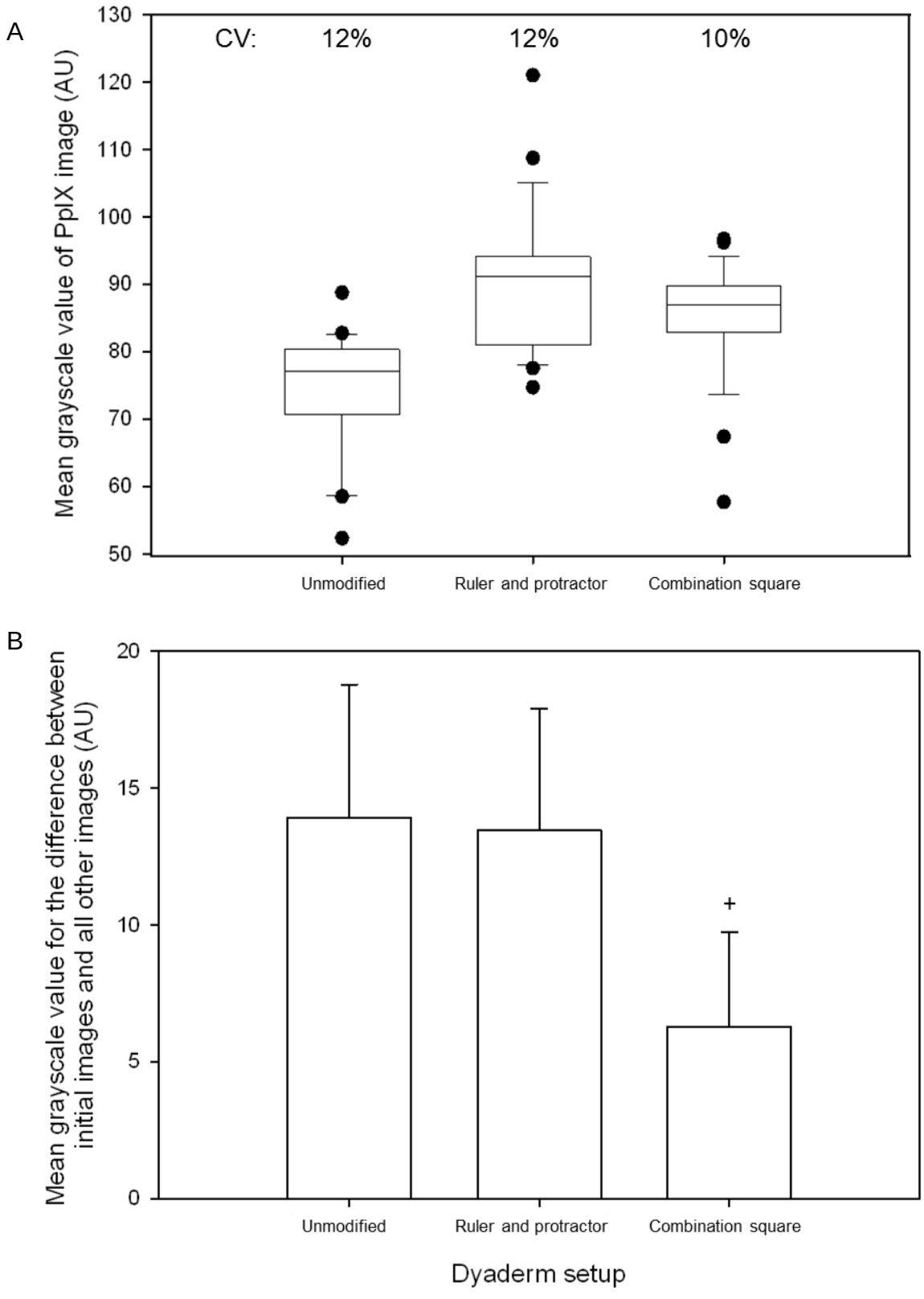
A
CV:
12%
12%
10%
Mean grayscale value of PpIX image (AU)
130
120
110
100
90
80
70
60
50
Unmodified
Ruler and protractor
Combination square
B
Mean grayscale value for the difference between initial images and all other images (AU)
20
15
10
5
0
+
Unmodified
Ruler and protractor
Combination square
Dyaderm setup

Figure 9

A

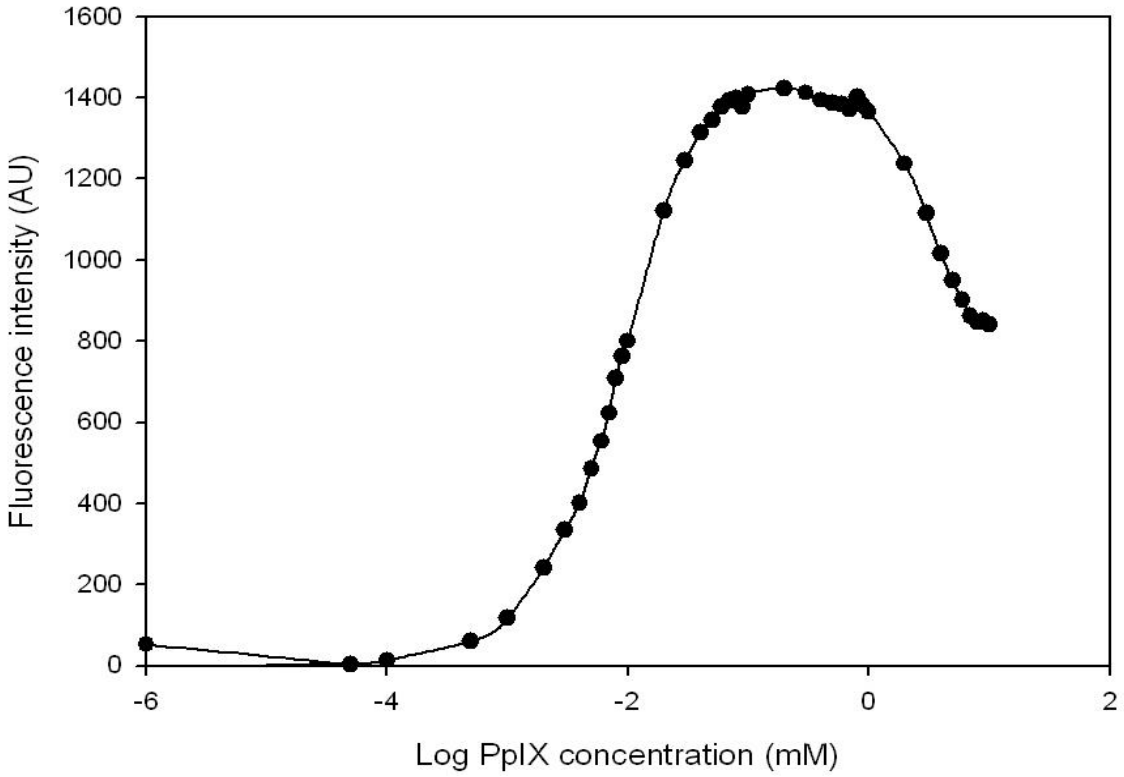
1600
1400
1200
1000
800
600
400
200
0
Fluorescence intensity (AU)
-6
-4
-2
0
2
Log PpIX concentration (mM)

B

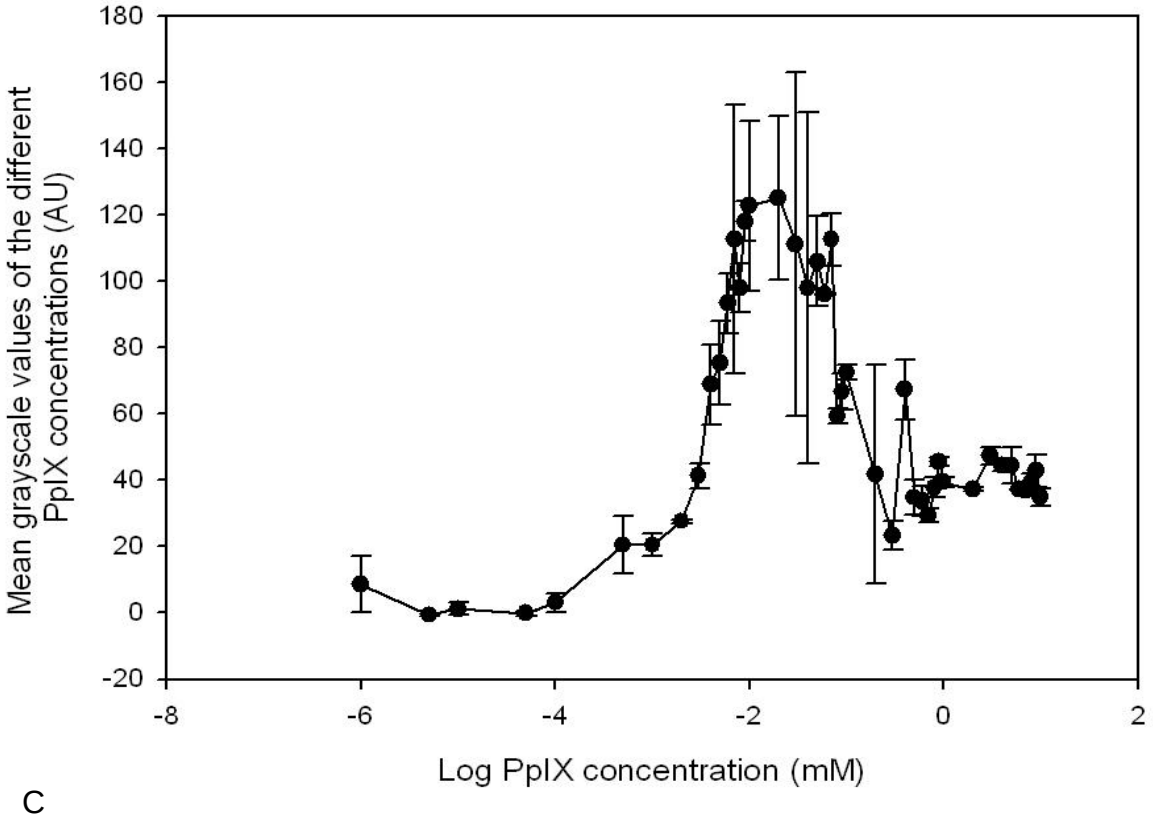
Mean grayscale values of the different PpIX concentrations (AU)
180
160
140
120
100
80
60
40
20
0
-20
-8
-6
-4
-2
0
2
Log PpIX concentration (mM)

C

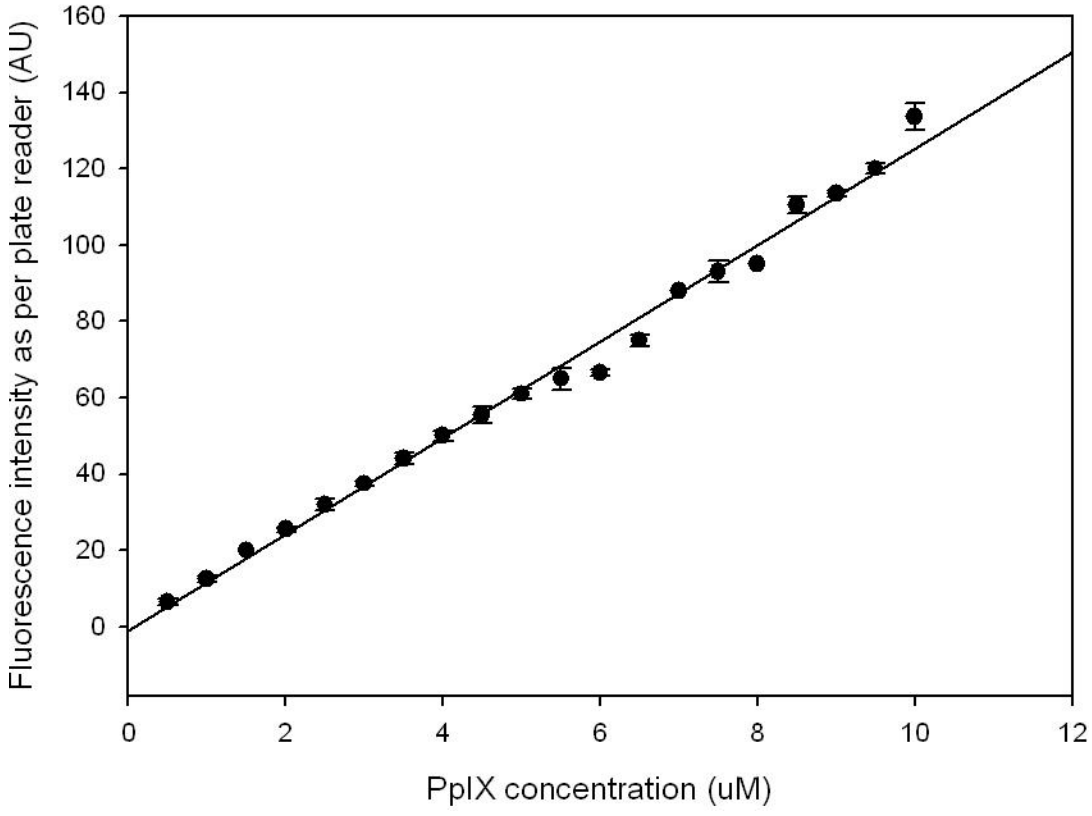
Fluorescence intensity as per plate reader (AU)
160
140
120
100
80
60
40
20
0
0
2
4
6
8
10
12
PpIX concentration (uM)

D

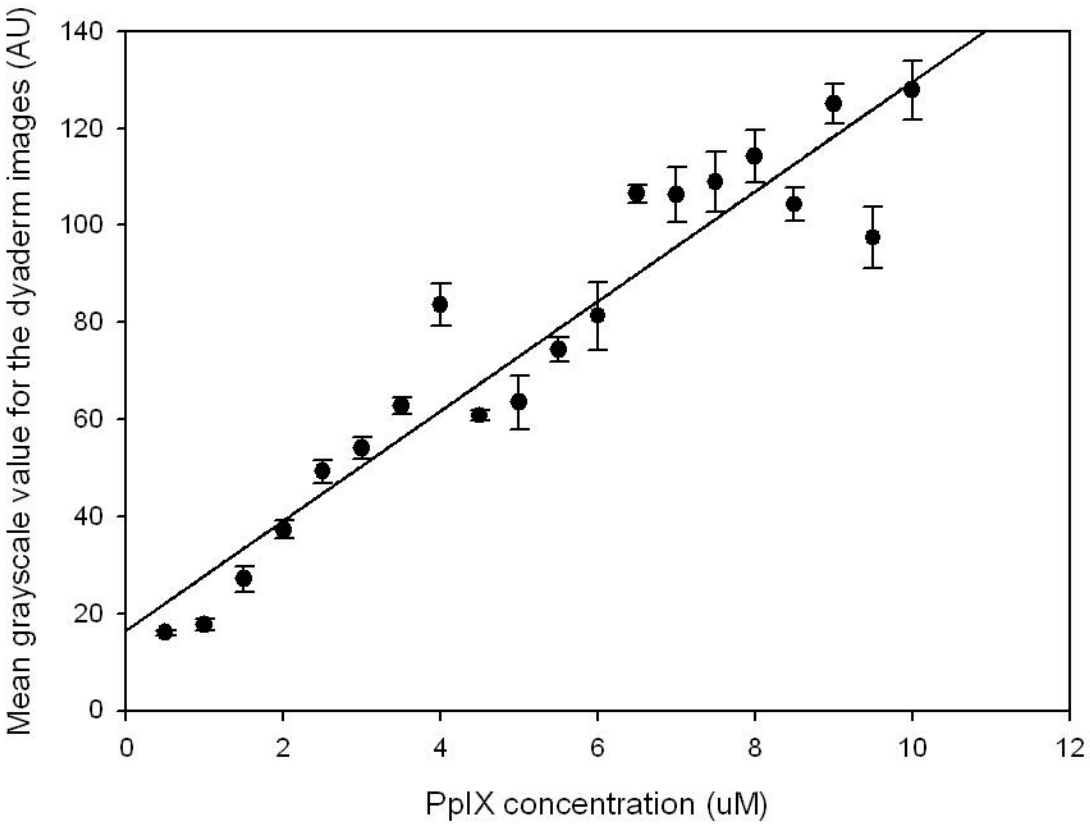

Figure 10

A

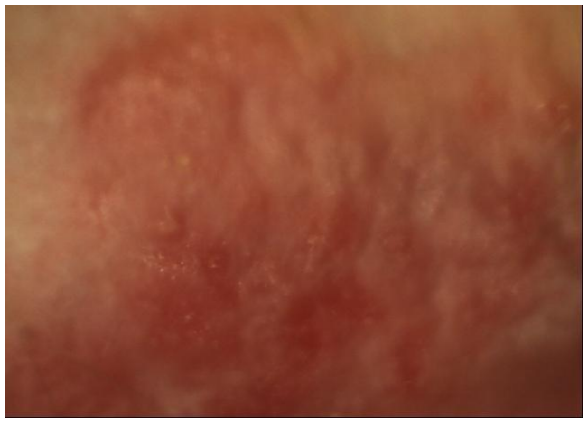

B

C

D

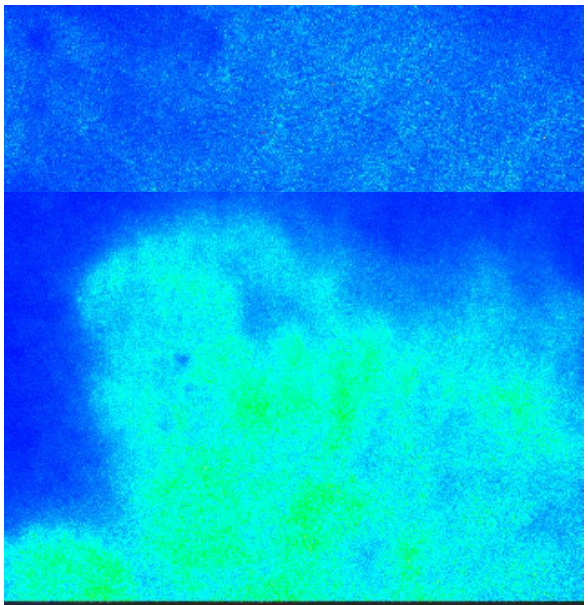

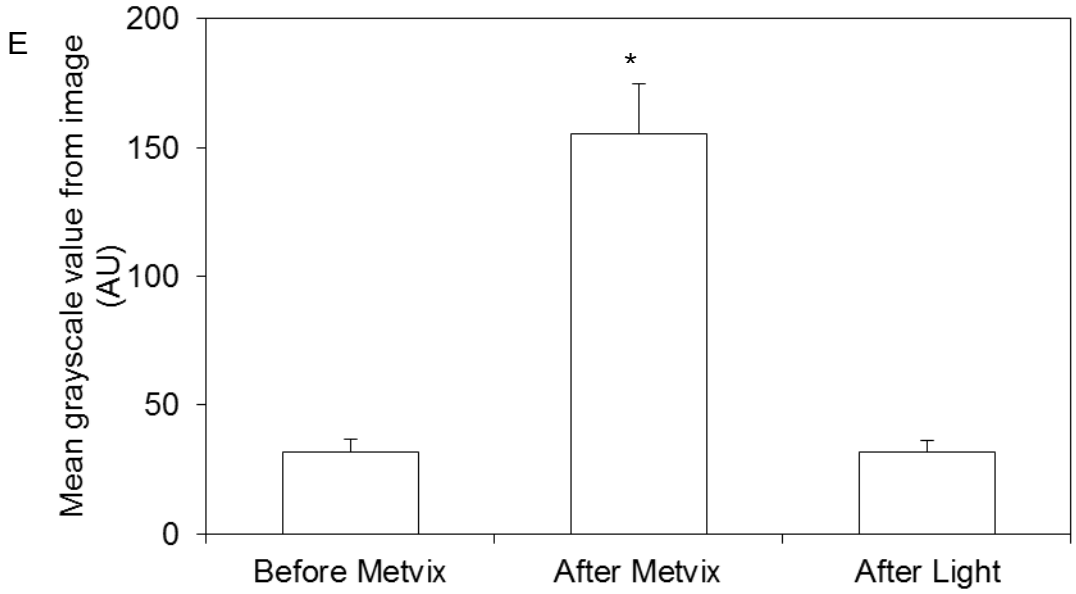
E
Mean grayscale value from image (AU)
200
150
100
50
0
*
Before Metvix
After Metvix
After Light

Figure 11

A

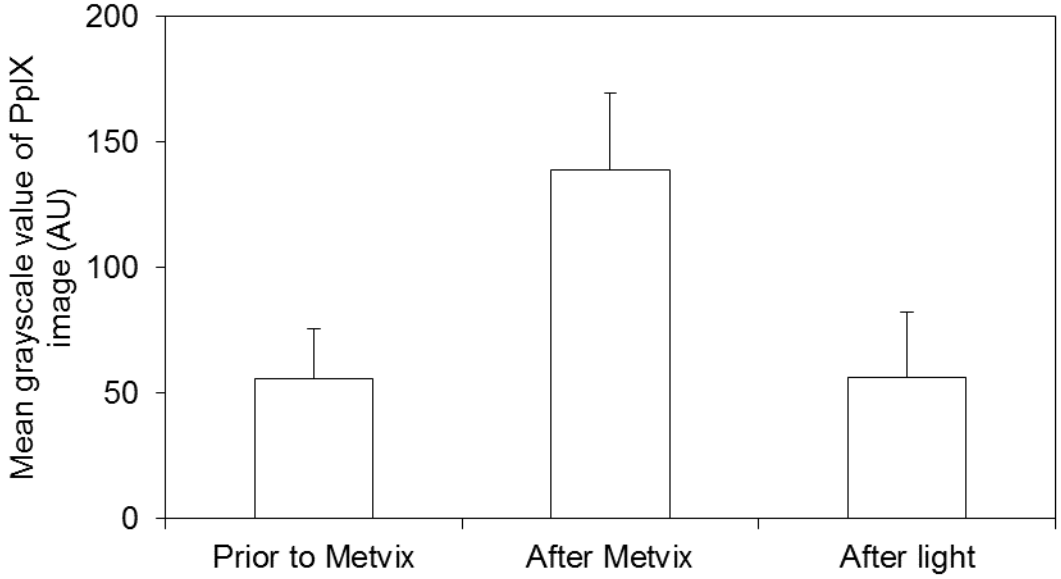
Mean grayscale value of PpIX image (AU)
200
150
100
50
0
Prior to Metvix
After Metvix
After light

B

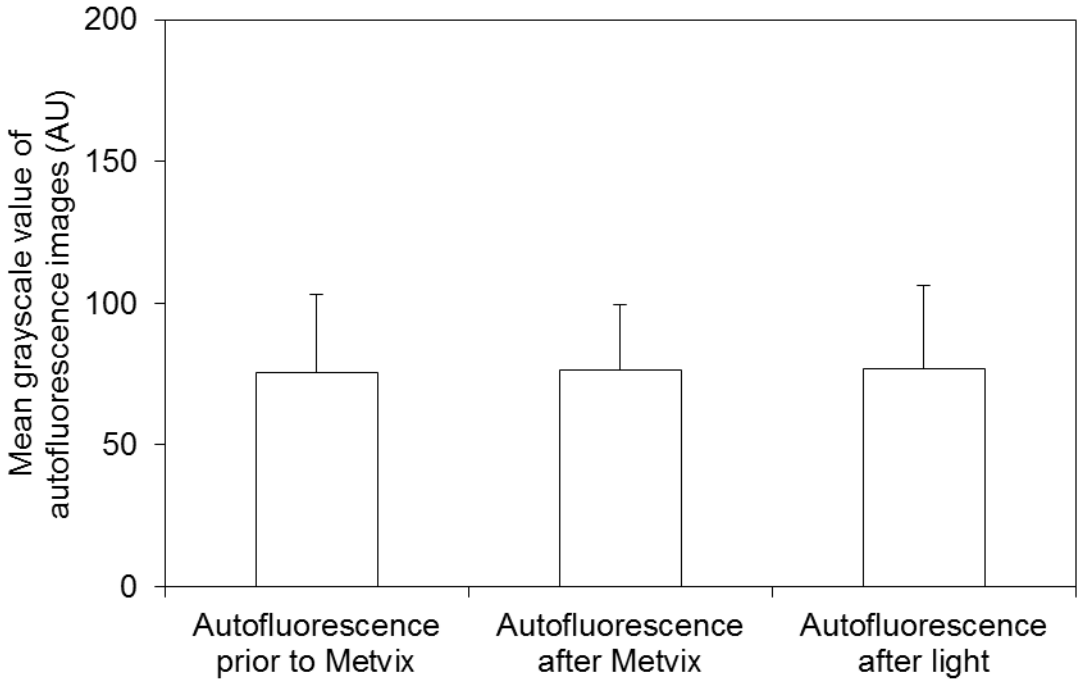
Mean grayscale value of autofluorescence images (AU)
200
150
100
50
0
Autofluorescence prior to Metvix
Autofluorescence after Metvix
Autofluorescence after light

Figure 12